August, 2015

Improved Detection by Ensemble-Decision Aliquot Ranking of Circulating Tumor Cells with Low Numbers of a Targeted Surface Antigen

Eleanor S. Johnson, *University of Washington - Seattle Campus*
Robbyn K. Anand, *University of Washington - Seattle Campus*
Daniel T. Chiu, *University of Washington - Seattle Campus*

analytical chemistry

Article

pubs.acs.org/ac

Improved Detection by Ensemble-Decision Aliquot Ranking of Circulating Tumor Cells with Low Numbers of a Targeted Surface Antigen

Eleanor S. Johnson, Robbyn K. Anand, and Daniel T. Chiu*

Department of Chemistry, University of Washington, Box 351700, Seattle, Washington 98195-1700, United States

Supporting Information

ABSTRACT: Circulating tumor cells (CTCs) are shed from a solid tumor into the bloodstream and can seed new metastases. CTCs hold promise for cancer diagnosis and prognosis and to increase our understanding of the metastatic process. However, their low numbers in blood and varied phenotypic characteristics make their detection and isolation difficult. One source of heterogeneity among CTCs is molecular: When they leave the primary tumor, these cells must undergo a molecular transition, which increases their mobility and chance of survival in the blood. During this molecular transition, the cells lose some of their epithelial character, which is manifested by the expression of the cell surface antigen known as epithelial cell adhesion molecule (EpCAM). Some tumors shed CTCs that express high levels of EpCAM; others release cells that have a low level of the antigen. Nevertheless, many CTC isolation techniques rely on the detection of EpCAM to discriminate CTCs from other cells in the blood. We previously reported a high-throughput immunofluorescence-based technology that targets EpCAM to rank aliquots of blood for the presence or absence of a CTC. This technology, termed ensemble decision aliquot ranking (eDAR), recovered spiked-in cancer cells (taken from a model EpCAM^{high} cell line) from blood at an efficiency of 95%. In this paper, we evaluated eDAR for recovery of cells that have low EpCAM expression and developed an immunofluorescence labeling strategy that significantly enhances the method's performance. Specifically, we used a cocktail of primary antibodies for both epithelial and mesenchymal antigens as well as a dye-linked secondary antibody. The cocktail allowed us to reliably detect a model EpCAM^{low} cell line for triple negative breast cancer, MDA-MB-231, with a recovery efficiency of 86%. Most significantly, we observed an average of 6-fold increase in the number of CTCs isolated from blood samples from breast cancer patients. These findings underscore the importance of benchmarking CTC technologies with model cell lines that express both high and low levels of EpCAM.

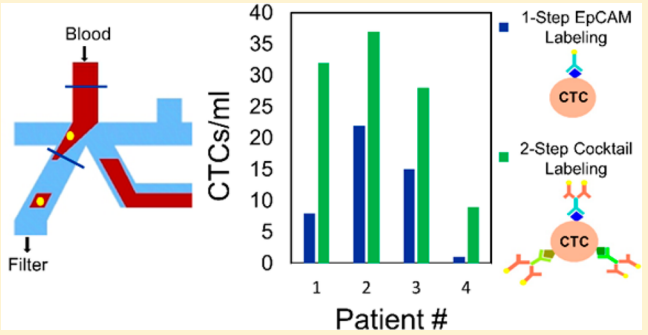

Circulating tumor cells (CTCs) escape the primary tumor site and enter the bloodstream. As their presence has been linked with metastasis and reduced patient survival,[1] CTCs serve as an important diagnostic and prognostic tool. However, despite much research effort, the low levels in whole blood (<10 CTCs/mL),[2−4] combined with their heterogeneity,[5] has made it difficult to detect CTCs consistently in patients. There are several methods for detecting and isolating CTCs, including flow cytometry,[6−8] immunomagnetic enrichment,[9,10,5] negative selection (depletion of white blood cells),[11] and immunoaffinity binding.[12−15] Many detection methods take advantage of the epithelial origin of CTCs, which provides the cells with surface markers that are distinct from those on other cells in the blood. However, for a tumor cell to migrate into the bloodstream, it is reported to undergo an epithelial-to-mesenchymal transition (EMT), losing some of its epithelial characteristics, such as structural rigidity, cell adhesion, and epithelial markers, such as EpCAM and cytokeratin, and taking on a more mesenchymal phenotype.[16] The phenotypic changes undergone by CTCs during the metastatic process mean that these cells may not express high levels of the epithelial markers, such as EpCAM, that are targeted by current CTC detection techniques. These "EpCAM^{low}" CTCs recently have received attention because they potentially can evade detection and have been linked with enhanced invasiveness and migration.[17] Accurate population statistics describing CTC expression of epithelial markers is unavailable. More importantly, immunoaffinity techniques traditionally quantify recovery rate (percentage of cells captured) using cultured cancer cells that are EpCAM^{high} (e.g., the breast cancer cell line MCF-7) thus leading to an *upper estimate* of CTC recovery.

Size-based separation platforms have been developed as alternatives that do not depend on antigen expression.[18−22]

Received: June 13, 2015
Accepted: August 22, 2015
Published: August 24, 2015

DOI: 10.1021/acs.analchem.5b02241
Anal. Chem. 2015, 87, 9389−9395

These methods are based on the principle that CTCs are typically larger than other cells in circulation and can be separated using filtration. As with antibody-based techniques, these methods work well with cultured cells and show high recoveries with spiked-in cell samples. However, these recovery rates usually come at a loss of purity since the size distributions of cancer and white blood cells sometimes are not very well separated.[23] CTCs in patient samples are quite heterogeneous in both size and expression of surface antigens so all detection methods will be biased and cause some CTCs to be missed. Importantly, it is not possible to fully simulate this heterogeneity with cultured cells that have not undergone the EMT. There are different ways to account for inherent bias, but the antibody-based approach offers more attractive options for expanding detection.

Previously, our group developed a highly sensitive CTC detection platform called eDAR, which stands for ensemble decision aliquot ranking. eDAR has been shown to be a robust platform for whole-blood isolation of rare cells present at levels as low as 1−10 cells/mL.[24] The platform uses laser-induced fluorescent (LIF) detection and microfluidic sorting of CTC-containing nanoliter-scale aliquots of whole blood (Figure 1).[24] In a side-by-side comparison with a commercial CTC-detection platform, CellSearch, eDAR detected CTCs in 82 out of 90 blood samples from stage IV breast cancer patients, while CellSearch detected CTCs in only 40 out of 90 samples.[25] Recoveries of spiked-in MCF-7 cells were 95%, with spike-in numbers between 10 to 100 cells per sample.[26]

In this paper, we targeted the detection and isolation of CTCs that express low levels of the target antigen epithelial cell adhesion marker, EpCAM, by combining eDAR with an enhanced immunofluorescence labeling strategy. Specifically, we used a cocktail of CTC-specific primary antibodies targeting both mesenchymal and epithelial cell surface markers as well as a single dye-linked secondary antibody. We demonstrated the detection of CTCs that otherwise would be missed by targeting EpCAM alone with a dye-linked primary antibody. We quantified the improved detection with both a model cell line that expresses low levels of EpCAM ($EpCAM^{low}$) spiked into whole blood and blood samples taken from breast cancer patients. The immunolabeling strategy is an important improvement over our previously published results as it addresses the heterogeneous nature of CTCs that makes them difficult to detect. The strategy also expands the limit of detection (LOD) in a quantifiable manner, which is important for accurate CTC counts in patient samples. There are two advantages of our two-step labeling strategy with more than one antibody: 1) The dye brightness from all of the targeted CTC markers is additive without an increase in the background fluorescence signal, and 2) Our chances of detecting CTCs are improved because any given CTC will robustly express at least one of the cell surface markers.

With our approach, we demonstrated an 86% recovery of cells from a model cell line and a 6-fold increase in the number of CTCs isolated from blood samples taken from three breast cancer patients. These results support the assertion that while $EpCAM^{high}$ cells provide a point of comparison between CTC isolation techniques, the recovery rates obtained are not necessarily representative of true CTC recovery rates, especially for patients with a significant proportion of $EpCAM^{low}$ CTCs.

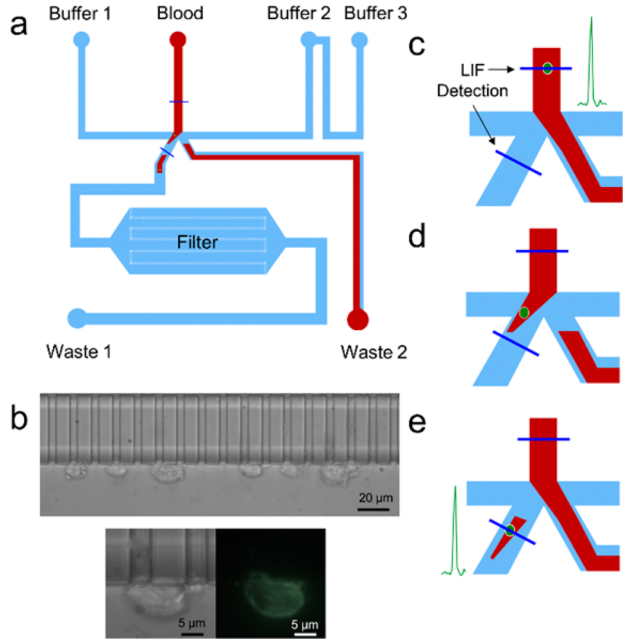

Figure 1. a An eDAR chip. The sample inlet (labeled "Blood") led to two outlets for collection—a microfluidic filter (labeled "Filter") for the capture of aliquots containing CTCs and a waste outlet for aliquots without CTCs (labeled "Waste 2"). A separate outlet (labeled "Waste 1") served to keep a constant buffer flow across the filter area. The solid blue lines indicate the location of laser lines incident on the inlet channel (upper line) and collection channel (lower line) of the eDAR chip. These laser lines are used for laser-induced fluorescence (LIF) detection of fluorescently tagged CTCs. **b** Images taken of PE-anti-EpCAM-labeled cultured cells (MCF-7) captured on the eDAR filter both in bright field (top and bottom left) and fluorescence (bottom right). The filter is used to retain the cells for visually confirming the identity of sorted cells of interest based on the expression of epithelial markers (EpCAM and cytokeratin), a nuclear stain (DAPI), and the absence of leukocyte marker (CD45). **c-d** An enhanced view of the eDAR sorting junction to describe the microfluidic sorting process. When a cell is detected at the upper LIF detection line (**c**), the avalanche photodiode (APD) detects a peak in signal intensity (shown at right). This event triggers actuation of a solenoid positioned in line with buffer line 2, causing the flow to increase from the right and the stream of blood to move to the left outlet (**d**), creating an aliquot of blood with the cell of interest. The solenoid then turns off and flow returns to normal. (**e**) Finally, the aliquot passes by a second LIF detection line (the lower line) to confirm the sort.

MATERIALS AND METHODS

Cell Culture. MCF-7 and MDA-MB-231 cell lines were obtained from American Type Culture Collection (ATCC, Manassas, VA). Cell lines were cultured at 37 °C and 5% CO_2 in EMEM and DMEM media (ATCC), respectively. Media was supplemented with 5% v/v fetal bovine serum (FBS) and 1% v/v penicillin streptomycin (both from Sigma, St Louis, MO).

Clinical Samples. Healthy whole blood was obtained from PlasmaLab International (Everett, WA). The samples of peripheral blood from breast cancer patients were obtained from NWBioTrust (Seattle, WA), using a protocol approved by the University of Washington Internal Review Board. All blood samples were collected in BD Vacutainer EDTA tubes (Franklin Lakes, NJ). Blood was processed within 2 days of collection and stored at 4 °C.

Reagents. Antibodies were purchased from BioLegend, Inc. (San Diego, CA) with the exception of phycoerythrin (PE)-

DOI: 10.1021/acs.analchem.5b02241
Anal. Chem. 2015, 87, 9389−9395

anti-EpCAM (Abcam, Cambridge, MA). Cell fixation buffer and permeabilization (saponin) buffer were obtained from BioLegend and Sigma, respectively. The saponin solution was made at 1 wt %/wt in Milli-Q water (EMD Millipore, Billerica, MA) and used at a final working concentration of 0.1%. Cell staining buffer for flow cytometry was purchased from BioLegend. Isoton II buffer, used as a sheath flow for eDAR, was purchased from Beckman Coulter (Brea, CA). PE-labeled calibration beads (BD Quantibrite PE beads) for flow cytometry were purchased from BD Biosciences (Franklin Lakes, NJ).

Microfluidic Chips. Silicon masters were made as described previously.[3] Briefly, silicon masters were made using standard photolithographic techniques including deep reactive ion etching to define the on-chip in-plane slit filter. Chips were made from PDMS in a 1:10 ratio of precursor to polymer base, fully cured, and sealed to a glass substrate immediately following exposure to O_2 plasma for 1 min. If not used immediately, chips were covered and stored until use but not longer than 1 week.

Flow Cytometry. For flow cytometry analysis, ~1×10^6 cells were labeled in 1 mL labeling buffer, made with 1×PBS, 3% FBS, and 0.1% NaN_3 (Sigma), with 0.1× of the manufacturer's recommended labeling concentration of antibodies. This concentration was determined to provide optimal cell labeling by a binding curve analysis (see Supporting Information, Figure S1). Cells were labeled for 1 h and then washed in 4 mL labeling buffer. Each of the washed cell-sample pellets and the PE calibration beads were separately resuspended in 1 mL labeling buffer each immediately prior to flow cytometry analysis. Isotype controls were performed in flow cytometry to confirm specificity of primary antibody binding (see Supporting Information, Figure S2). FACS Scan and LSRII flow cytometers were used for all flow cytometry analysis at the University of Washington Cell Analysis facility. Data was analyzed using FlowJo (Ashford, OR) to obtain the geometric mean fluorescence intensity (FL2, 585/12 filter) of each cell population. A calibration curve obtained with the PE beads was used to convert these intensities to antibodies bound per cell (ABC).

eDAR Detection of Spiked-in Cultured Cells. Approximately 200,000 cells were pipetted into 100-μL Isoton. Next, 1 mL of whole blood was pipetted on top of the Isoton. Finally, 0.1× of the recommended concentration of each antibody was added to the blood and incubated in the dark, at room temperature (21 °C) on a rocker for 1 h. After incubation, samples were washed with 12 mL Isoton and centrifuged at 890 RCF for 10 min. The supernatant was removed to the original 1 mL volume carefully, so as not to disturb the cells. For the two-step labeling scheme, the secondary antibody (0.1× recommended concentration) was added to the washed blood at this time. The incubation and washing steps were repeated. After completion of labeling, samples were processed within 2 h. Using a syringe pump, samples were introduced into the sample inlet of the eDAR chip at a flow rate of 50 μL/min, and a fluorescence intensity trace from avalanche photodiodes (APDs) was collected for at least 5 min to obtain 50,000 data points. Excitation of the fluorescently labeled cells was achieved using a 488 nm laser. The resulting epi-fluorescence signal was divided into red, green, and yellow components and collected at APDs. The signal from the yellow channel was analyzed using MATLAB to obtain histograms of the fluorescence intensities of the population of labeled cells. Antigen expression levels of these cells were determined by analyzing paired cell samples in flow cytometry with calibration beads. We found calibration in flow cytometry to be more accurate in determining antigen expression level on spiked-in cells than using the calibration beads in the eDAR chip. Using this method, we were able to analyze the eDAR response (fluorescence intensity peak area) in terms of PE-labeled antibodies bound for each cell population. By plotting the geometric mean intensities in eDAR versus those found in flow cytometry for several cell populations, we obtained a limit of detection (LOD) for eDAR of 5800 PE-labeled ABC (Antibody Bound per Cell). More details about the data analysis can be found in the Supporting Information.

eDAR Isolation of CTCs from Patient-Derived Samples. To verify the hypothesis that the enhanced labeling scheme yielded higher recovery rates of CTCs, we analyzed paired blood samples, one labeled with PE-anti-EpCAM alone and one labeled with the cocktail scheme. The breast cancer samples we obtained for our study were classified based on the primary tumor expression of estrogen receptor (ER), progesterone receptor (PR), and human epidermal growth factor receptor 2 (HER2), as well the stage of the cancer (1−4). The four patients were classified as follows: patient 1 was stage 3, ER+PR+HER2-; patient 2 was stage 4, ER+PR-HER2+; patient 3 was stage 2, ER+PR+HER2-; and patient 4 was stage 2, ER+PR-HER2-. The labeling process and eDAR recovery of CTCs followed previously reported protocols.[26] Briefly, 2 mL of whole blood was labeled with fluorescently labeled antibodies for 1 h and washed with 12 mL Isoton. The sample was then centrifuged at 890 RCF for 10 min, and the supernatant was removed to obtain the original 2 mL volume. Once fully labeled, blood was loaded into a syringe and introduced into an eDAR chip (Figure 1a) at 50 μL/min. Sorting was established by adjusting the sheath flow pressures until blood flowed to the Waste 2 reservoir when an in-line solenoid was closed and to the filter when it was open (Figure 1 c-e). Aliquots of blood were sorted based on the presence or absence of a fluorescence signal when passing a laser-induced fluorescence (LIF) detection line, with positive aliquots going to a microfluidic filter with 5 μm slits for further analysis and negative aliquots being sent to Waste 2. In the one-step EpCAM scheme, blood was labeled with PE-anti-EpCAM for 1 h. In the two-step scheme, first, a cocktail of primary antibodies comprised of bare mouse-antihuman EpCAM, EGFR, HER2, and N-cadherin was added to the blood and labeled for 1 h. After a washing step, the sample was labeled with the secondary antibody, PE-goat-antimouse-IgG, for 1 h. The sample was washed again prior to being processed on eDAR. Blood from breast cancer patients was analyzed by eDAR within 2 days of being drawn.

After the whole volume of blood was sorted by eDAR, postsorting labeling of the captured cells was carried out. Fixation and permeabilization buffers as well as the dye-linked antibodies were introduced to the capture area (slit filter) using a peristaltic pump (MiniPump, Variable Flow, Fisher). In this process, the fixation solution was flowed onto the chip, incubated for 10 min, and rinsed. Then, permeabilization buffer along with Alexa647-antipancytokeratin, DAPI (nuclear stain), and Alexa700-anti-CD45 (all from BioLegend) were flowed onto the on-chip filter and incubated for 30 min. Images were taken using a CCD camera (Model GC1380, Allied Vision, Exton, PA). The imaged cells were evaluated for CTC characteristics. The criteria for CTC identification were that

DOI: 10.1021/acs.analchem.5b02241
Anal. Chem. 2015, 87, 9389−9395

the cells were EGFR$^+$, HER2$^+$, N-cadherin$^+$, EpCAM$^+$, or cytokeratin$^+$, and CD45$^-$ with positive nuclear stain.

RESULTS AND DISCUSSION

eDAR Detection of a Model EpCAM^{low} Cell Line. A population of CTCs can have widely varied phenotypic characteristics because of the changes CTCs undergo as they escape from solid tumor tissue and enter the bloodstream. Most notably, CTCs from tumors of epithelial origin shed their epithelial phenotypic traits to differing degrees and assume mesenchymal hallmarks (a phenomenon known as EMT). Therefore, researchers can anticipate a wide distribution of expression levels for epithelial biomarkers, including the most common antigen targeted for CTC detection − EpCAM. Despite the variability in EpCAM expression, the prevailing method for benchmarking CTC isolation techniques is to spike EpCAM^{high} cultured cancer cells, typically MCF-7 or SKBr3 for breast cancer, into a sample of healthy blood. This approach provides inadequate information to determine the dependence of each technique's performance on the target cells' expression level of EpCAM. Cells that have undergone the EMT (and are therefore EpCAM^{low}) are known to be more capable of survival in the bloodstream and more invasive. Therefore, it is critical to characterize the ability of a technique to isolate EpCAM^{low} cells.

To demonstrate the impact of heterogeneity in EpCAM expression on CTC detection, we benchmarked eDAR performance using two cell lines with known EpCAM expression levels—MDA-MB-231 (EpCAM^{low}) and MCF-7 (EpCAM^{high}). The MDA-MB-231 cell line expresses approximately 10,000−15,000 EpCAM/cell, and the MCF-7 cell line expresses approximately 100,000−500,000 EpCAM/cell based on flow cytometry analysis (three trials separated by several weeks). Previously, we demonstrated greater than 95% recovery of MCF-7 cells spiked into whole blood.[26] To evaluate the performance of eDAR for detection of EpCAM^{low} cells, approximately 3.0×10^4 MDA-MB-231 cells were spiked into 1 mL of blood and labeled with PE-anti-EpCAM. The entire volume of blood was flowed through the eDAR chip, and the resulting fluorescence intensity trace was analyzed using an in-house peak recognition algorithm in MATLAB to count the percentage of cells detected. This approach yielded a detection rate of ∼20%, which indicates that the majority of the cells fell below the LOD of eDAR.

Initial progress toward detecting these EpCAM^{low} cells was made by moving to a two-step scheme. This detection scheme consisted of a bare primary anti-EpCAM antibody followed by a PE-conjugated secondary antibody (Figure 2a and 2b). The strategy resulted in a 2- to 3-fold increase in brightness (Figure 2c) caused by multiple fluorescent secondary antibodies binding to each anti-EpCAM primary antibody. By this improvement alone, the detection rate for MDA-MB-231 cells increased to 60%. While nearly 85% of the cells were above the LOD of eDAR (Figure 2c), our threshold for sorting most practically was set at or slightly below the limit of quantitation (10σ above the average background, where σ is the standard deviation of the noise) due to fluctuations in the background fluorescence of the blood sample. Therefore, with the goal of capturing the majority of EpCAM^{low} cells, we sought to further improve our labeling strategy.

To circumvent the limitations of the eDAR LIF detection scheme and to take advantage of the inherent brightness of PE-labeled antibodies, we decided to use a cocktail of antibodies all carrying the same fluorescent tag to generate an additive signal.

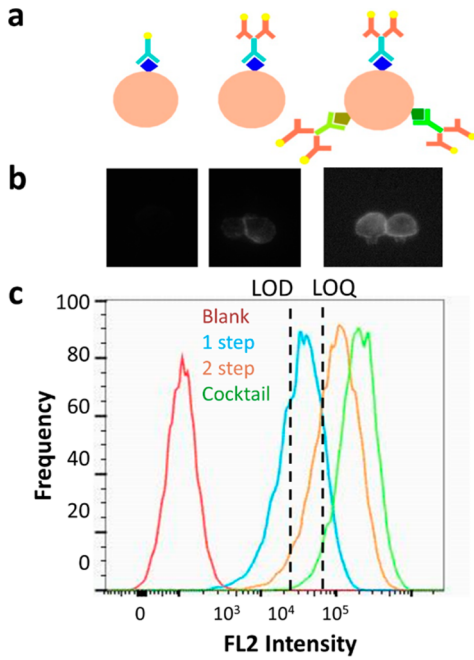

Figure 2. **a** Scheme of the three labeling strategies used: 1-step EpCAM, 2-step EpCAM, 2-step cocktail (from left to right). **b** Images of MDA-MB-231 cells labeled with each of the three strategies. **c** Flow cytometry histogram of the fluorescence intensities of MDA-MB-231 cells employing each of the three labeling strategies. The LOD (limit of detection) and LOQ (limit of quantification) of eDAR in terms of the number of PE molecules bound per cell are indicated by the dashed lines.

This cocktail was designed to incorporate antibodies against both epithelial and mesenchymal markers to account for CTC heterogeneity. However, a cocktail of fluorescently tagged primary antibodies yielded an unacceptable increase in background fluorescence in the blood. The problem arose from the postlabeling washing protocol: After mixing the labeled blood with Isoton buffer, the sample was centrifuged, and the supernatant was pipetted off down to the original volume of whole blood (e.g., 1 mL). Therefore, there were residual unbound fluorescently tagged antibodies in the retained fraction. We overcame this problem by using a cocktail of bare primary antibodies followed by a single dye-linked secondary antibody. With this approach, the fluorescence background was only affected by the concentration of secondary antibody and was independent of the number of unique primary antibodies in the cocktail.

The antigens targeted by the cocktail were EpCAM, EGFR, HER2, and N-cadherin. EpCAM and EGFR are epithelial markers most often found on epithelial tumors. HER2 was included in anticipation of the analysis of clinical samples from breast cancer patients because HER2 is overexpressed in some types of breast cancer. We decided to use anti-HER2 labeling in all of our clinical samples (including those classified as HER2$^-$) because there is evidence that even patients with HER2$^-$ status can have HER2$^+$ CTCs.[27] N-cadherin is a mesenchymal marker that has been noted in CTCs that have undergone the EMT.[28] Its inclusion in the cocktail was useful for the recovery of cells lacking epithelial characteristics.

The cocktail scheme was evaluated as follows. First, 3.0×10^4 MDA-MB-231 cells were spiked into 1 mL of blood. Second, the blood was incubated for 1 h with the cocktail of primary mouse-derived antibodies against EpCAM, EGFR, HER2, and

DOI: 10.1021/acs.analchem.5b02241
Anal. Chem. 2015, 87, 9389−9395

N-cadherin and then washed. The sample was incubated for 1 h with PE-goat-antimouse IgG and washed. Finally, the entire sample volume was flowed through the eDAR chip, and the resulting fluorescence intensity trace was analyzed. The detection rate of our approach was determined to be 86%.

Much of the observed improvement in detection rate was because the MDA-MB-231 cell line was EGFR positive. This result does not demonstrate enhanced detection of biomarkers that are underexpressed. However, the experiment illustrates the strength of the cocktail approach, which was further underscored by flow cytometry data (see SI Figure S3) that shows the intensity of MDA-MB-231 cells labeled for all biomarkers was the sum of that measured for each individual marker.

Quantitative Approach to eDAR Recovery Efficiency. A significant advantage of eDAR over other CTC detection and isolation methods is that LIF detection lends itself to the quantification of targeted antigens. Other CTC isolation techniques can be limited in this regard; for example, when cells were captured by immunoaffinity binding of cells to an antibody-coated substrate,[29] a truly quantitative analysis of device performance versus antigen expression level would involve complex calculations that incorporate binding affinity, flow profiles, and cell characteristics. The only practical method for comparing CTC techniques to each other is to count the number of spiked-in cultured cancer cells recovered from a blood sample. MCF-7 ($EpCAM^{high}$) cells are typically used. However, eDAR does not share in this limitation because the impact of antigen expression on capture efficiency can be independently quantified.

There are a number of steps in eDAR that contribute to the overall recovery rate of the system, with each step having a distinct probability for CTC loss. These steps include the following: 1) sample processing (labeling, washing, and transfer steps), 2) CTC detection by LIF, 3) CTC capture on the filter, and 4) confirmation by imaging. The probability of CTC loss is not easily described at all of these steps. However, we do know that for $EpCAM^{high}$ cells, the recovery efficiency averages 95%. We can assume when we work with cells with lower EpCAM expression levels that the losses from steps 1, 3, and 4 remain constant, but the loss from step 2 (LIF detection) decreases with decreased cell brightness. Once the LIF detection is well characterized, separate spike-in and recovery experiments are not required to calculate recovery efficiency for new labeling schemes or cell types. Therefore, we can forecast the recovery efficiency for any cell population with a known distribution of antigen expression.

A related advantage of the eDAR format is that it lends itself to spike-in studies with a statistically relevant number of cells (tens of thousands). Figure 3a shows histograms for four different cell populations derived from eDAR fluorescence intensity traces. The histograms were plotted using the log of peak area for each event on the trace going above a cutoff threshold (above 6σ). The four cell populations were comprised of two cell types, each processed by the two labeling schemes. These four eDAR samples were prepared as follows. First, each cell population was labeled in cell labeling buffer and subsequently divided into two portions (the first portion for eDAR and the second for flow cytometry). For eDAR, a total of 30,000−40,000 cells from each population was spiked into four separate 1 mL blood samples and then flowed through the eDAR chip as the intensity trace was recorded. Importantly, these blood samples were prewashed (before

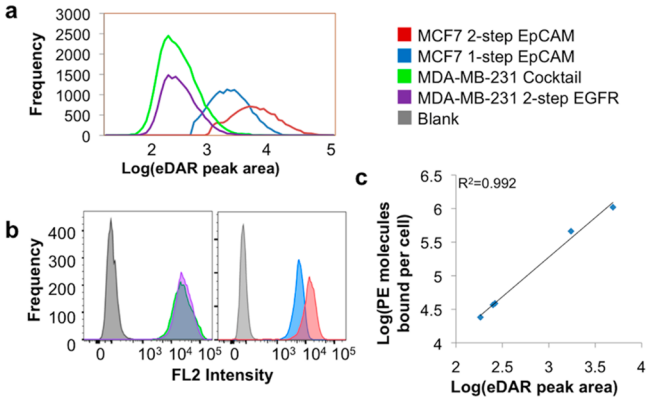

Figure 3. a Histogram showing the distribution of cell brightness from the four cell populations measured in eDAR. The four populations were labeled and spiked into blood for eDAR analysis or into buffer for flow cytometry analysis. **b** Flow cytometry histograms of the same four populations. **c** Plot of the geometric mean intensities of the four cell populations comparing the number of PE molecules bound to the peak area measured in eDAR. The high R^2 value indicates that eDAR is quantitative with respect to antigen expression and that the modes from eDAR and flow cytometry can be used to determine the LOD.

spiking in cells) to account for the processing that occurs during eDAR analysis of a clinical sample. Of these four populations, MDA-MB-231 cells labeled for EGFR by the 2-step scheme were the dimmest, while the MCF-7 cells labeled for EpCAM by the 2-step scheme were the brightest. For the brightest population, a neutral density filter was required to bring the fluorescence intensity down into the linear range of the APD. To characterize the number of PE molecules bound to the cells, the remaining second portion of the labeled cells was analyzed by flow cytometry, and the intensity was translated to the number of PE-linked ABC using PE calibration beads (Figure 3b).

The results demonstrate that the eDAR peak area is a quantitative measure of the number of PE-linked ABC. Specifically, the cell populations yielded similar distributions by eDAR and flow cytometry; when plotted against each other, the geometric mean intensities from both techniques yielded a straight line (Figure 3c, R^2 = 0.992). Using this data, we estimated for eDAR an LOD of 5,800 PE molecules per cell and a LOQ of 23,500 PE molecules per cell (see SI for discussion of LOD and LOQ determination). It should be noted that the LOQ is more relevant to CTC recovery rates than the LOD because under practical operating conditions, the sorting threshold for eDAR is usually set near the LOQ. As the fluorescence background from the blood sample fluctuates, sorting can be triggered in error, sending an excessive number of CTC-negative aliquots of blood to the filter. Defining an LOQ for eDAR is significant because it establishes a cutoff for CTC detection. An LOQ of 23,500 PE molecules/cell means that cells having 23,500 dye-linked ABC will be reliably detected and sorted.

Finally, the data underscore that eDAR is capable of providing quantitative data for biomarker expression levels falling within the linear range of detected intensities. While the current linear range of eDAR does not extend to sufficiently high intensities to quantify antigen expression on $EpCAM^{high}$ cells labeled using the 2-step scheme, the range can be extended to higher intensities simply by splitting off 1% of the signal to a separate APD. For many CTC technologies, quantitative data is

DOI: 10.1021/acs.analchem.5b02241
Anal. Chem. 2015, 87, 9389−9395

not obtained during the capture step. Some techniques, such as CellSearch, exploit EpCAM as a binding site for magnetically tagged antibodies and block these sites from further analysis.[9] Other techniques allow for downstream quantification of EpCAM during postsecondary labeling and imaging steps. However, postsecondary quantification of EpCAM is time-consuming. eDAR's ability to provide rapid quantitative measurements is significant because the expression level of EpCAM (or other biomarkers) on CTCs may prove to be clinically relevant.

6-Fold Increased Recovery of CTCs from Patient-Derived Samples. The relevance and success of the cocktail labeling scheme that we developed needed to be evaluated with clinical samples. To quantify the improvement, we compared the cocktail labeling scheme to our former labeling strategy of PE-anti-EpCAM alone. Figure 4a shows a bar graph with the number of CTCs isolated with each labeling scheme (cocktail and PE-anti-EpCAM) for each of the samples obtained from four breast cancer patients. Patient 1 was stage 3, ER+PR+HER2-; patient 2 was stage 4, ER+PR-HER2+; patient 3 was stage 2, ER+PR+HER2-; and patient 4 was stage 2, ER+PR+HER2-. In this experiment, each sample was divided into two 2 mL portions. The samples were analyzed by eDAR sequentially using each of the two labeling schemes. Samples were processed within 2 days after the blood was drawn. The data in Figure 4a demonstrate that a significant improvement, averaging 6×, was observed with the cocktail scheme. Figure 4b and c show representative cells that were isolated and further labeled against CD45, cytokeratin, and DAPI (postcapture) to confirm CTC identity.

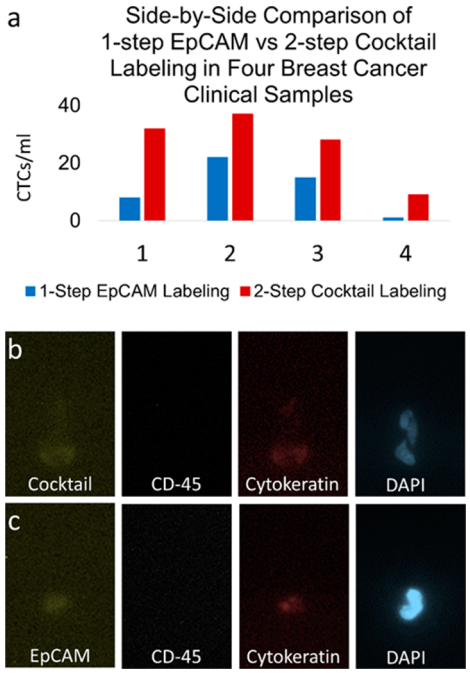

Figure 4. Cells from breast cancer clinical samples were sorted on an eDAR chip. Following sorting, the cells were fixed, permeabilized, and labeled with CD45-alexa700, Pancytokeratin-alexa647, and DAPI to verify whether the cells were CTCs. **a** Chart showing the number of CTCs recovered from each of the four clinical breast samples, where 2 mL of blood was run with each 1-step EpCAM and 2-step cocktail. Patient 1 was stage 3, ER/PR+HER2-, patient 2 was stage 4, ER+PR-HER2+, patient 3 was stage 2, ER/PR+HER2-, and patient 4 was stage 2, ER+PR+HER2-. **b.** Fluorescence images of a cell captured by eDAR using the cocktail labeling scheme (cocktail included primary bare anti-EpCAM, anti-EGFR, anti-HER2, and anti-N-Cadherin followed by secondary PE-goat-antimouse-IgG). **c** A cell detected using the 1-step PE-anti-EpCAM labeling scheme.

These results demonstrate a significant improvement in CTC recovery with our cocktail labeling scheme. They also validate the assertion that there are EpCAM^{low} CTCs in the blood of breast cancer patients. We increased the capability to isolate and characterize these EpCAM^{low} cells that represent a potentially more invasive population of CTCs. This enhanced sensitivity and selectivity can take advantage of our dual-filter sorting chip to isolate two distinct cell populations (high and low EpCAM expression) to separate on-chip filters.[30] Finally, we are in the process of developing downstream analytical tools to extract genetic and phenotypic information from the CTCs. The information will be critical in unraveling the mechanisms of metastasis and developing antimetastatic drugs.

CONCLUSION

We demonstrated the improved detection of CTCs in whole blood with a cocktail labeling scheme targeted against both epithelial and mesenchymal biomarkers. We validated the approach first with a model EpCAM^{low} cell line and then with samples taken from breast cancer patients. Detection rates for EpCAM^{low} cells were improved from 20% with our earlier eDAR protocol to 86%. More significantly, the number of CTCs recovered from the clinical samples was increased 6-fold. This improvement is particularly important in light of a growing body of research demonstrating both the prevalence and invasiveness of EpCAM^{low} CTCs.

We further demonstrated two distinct advantages of eDAR including: 1) ability to establish LOD and LOQ values for dye-linked ABC and antigen expression level and 2) quantitative data about CTCs' surface antigen expression levels during the detection step. Many CTC detection schemes are benchmarked solely based of recovered cells from spike-in samples. However, the most common cell line used in CTC technology development, MCF-7, expresses high levels of EpCAM, which is unlikely to represent all CTCs found in cancer patients. The ability to detect, isolate, and analyze the full spectrum of CTCs, including the frequently missed EpCAM^{low} cells, from patient samples poises eDAR for both improved cancer diagnostics and deeper study of cancer metastasis. Most significantly, eDAR may enable us to uncover the correlations between antigen expression and disease outcomes.

ASSOCIATED CONTENT

Supporting Information

The Supporting Information is available free of charge on the ACS Publications website at DOI: 10.1021/acs.analchem.5b02241.

Signal intensity and signal-to-noise evaluation and isotype control experiments; further description of eDAR calibration (PDF)

AUTHOR INFORMATION

Corresponding Author

*E-mail: chiu@chem.washington.edu.

Notes

The authors declare the following competing financial interest(s): D.T.C. has financial interest in MiCareo, which

DOI: 10.1021/acs.analchem.5b02241
Anal. Chem. 2015, 87, 9389−9395

has licensed the described technology from the University of Washington.

■ ACKNOWLEDGMENTS

We are grateful to the Department of Defense CDMRP Program (BC100510) for support of this work. R.K.A. received support from the grant T32CA138312 from the National Cancer Institute. The content is solely the responsibility of the authors and does not necessarily represent the official views of the National Cancer Institute or the National Institutes of Health.

■ REFERENCES

(1) Cohen, S. J.; Punt, C. J. A.; Iannotti, N.; Saidman, B. H.; Sabbath, K. D.; Gabrail, N. Y.; Picus, J.; Morse, M.; Mitchell, E.; Miller, M. C.; Doyle, G. V.; Tissing, H.; Terstappen, L. W. M. M.; Meropol, N. J. *J. Clin. Oncol.* **2008**, *26*, 3213−3221.
(2) Paterlini-Brechot, P.; Benali, N. L. *Cancer Lett.* **2007**, *253*, 180−204.
(3) Dharmasiri, U.; Witek, M. A.; Adams, A. A.; Soper, S. A. *Annu. Rev. Anal. Chem.* **2010**, *3*, 409−431.
(4) Alunni-Fabbroni, M.; Sandri, M. T. *Methods* **2010**, *50*, 289−297.
(5) Powell, A. A.; Talasaz, A. H.; Zhang, H.; Coram, M. A.; Reddy, A.; Deng, G.; Telli, M. L.; Advani, R. H.; Carlson, R. W.; Mollick, J. A.; Sheth, S.; Kurian, A. W.; Ford, J. M.; Stockdale, F. E.; Quake, S. R.; Pease, R. F.; Mindrinos, M. N.; Bhanot, G.; Dairkee, S. H.; Davis, R. W.; Jeffrey, S. S. *PLoS One* **2012**, *7*, e33788.
(6) Gross, H. J.; Verwer, B.; Houck, D.; Hoffman, R. A.; Recktenwald, D. *Proc. Natl. Acad. Sci. U. S. A.* **1995**, *92*, 537−541.
(7) Hsieh, H. B.; Marrinucci, D.; Bethel, K.; Curry, D. N.; Humphrey, M.; Krivacic, R. T.; Kroener, J.; Kroener, L.; Ladanyi, A.; Lazarus, N.; Kuhn, P.; Bruce, R. H.; Nieva, J. *Biosens. Bioelectron.* **2006**, *21*, 1893−1899.
(8) Krivacic, R. T.; Ladanyi, A.; Curry, D. N.; Hsieh, H. B.; Kuhn, P.; Bergsrud, D. E.; Kepros, J. F.; Barbera, T.; Ho, M. Y.; Chen, L. B.; Lerner, R. A.; Bruce, R. H. *Proc. Natl. Acad. Sci. U. S. A.* **2004**, *101*, 10501−10504.
(9) Allard, W. J.; Matera, J.; Miller, M. C.; Repollet, M.; Connelly, M. C.; Rao, C.; Tibbe, A. G. J.; Uhr, J. W.; Terstappen, L. W. M. M. *Clin. Cancer Res.* **2004**, *10*, 6897−6904.
(10) Riethdorf, S.; Müller, V.; Zhang, L.; Rau, T.; Loibl, S.; Komor, M.; Roller, M.; Huober, J.; Fehm, T.; Schrader, I.; Hilfrich, J.; Holms, F.; Tesch, H.; Eidtmann, H.; Untch, M.; von Minckwitz, G.; Pantel, K. *Clin. Cancer Res.* **2010**, *16*, 2634−2645.
(11) Balasubramanian, P.; Yang, L.; Lang, J. C.; Jatana, K. R.; Schuller, D.; Agrawal, A.; Zborowski, M.; Chalmers, J. J. *Mol. Pharmaceutics* **2009**, *6*, 1402−1408.
(12) Nagrath, S.; Sequist, L. V.; Maheswaran, S.; Bell, D. W.; Ryan, P.; Balis, U. J.; Tompkins, R. G.; Haber, D. A. *Nature* **2007**, *450*, 1235−1239.
(13) Dharmasiri, U.; Njoroge, S. K.; Witek, M. A.; Adebiyi, M. G.; Kamande, J. W.; Hupert, M. L.; Barany, F. *Anal. Chem.* **2011**, *83*, 2301−2309.
(14) Wang, S.; Liu, K.; Liu, J.; Yu, Z. T. F.; Xu, X.; Zhao, L.; Lee, T.; Lee, E. K.; Reiss, J.; Lee, Y. K.; Chung, L. W. K.; Huang, J.; Rettig, M.; Seligson, D.; Duraiswamy, K. N.; Shen, C. K. F.; Tseng, H. R. *Angew. Chem., Int. Ed.* **2011**, *50*, 3084−3088.
(15) Yu, L.; Ng, S. R.; Xu, Y.; Dong, H.; Wang, Y. J.; Li, C. M. *Lab Chip* **2013**, *13*, 3163−3182.
(16) Kalluri, R.; Weinberg, R. A. *J. Clin. Invest.* **2009**, *119*, 1420−1428.
(17) Driemel, C.; Kremling, H.; Schumacher, S.; Will, D.; Wolters, J.; Lindenlauf, N.; Mack, B.; Baldus, S. A.; Hoya, V.; Pietsch, J. M.; Panagiotidou, P.; Raba, K.; Vay, C.; Vallböhmer, D.; Harréus, U.; Knoefel, W. T.; Stoecklein, N. H.; Gires, O. *Oncogene* **2014**, *33*, 4904−4915.
(18) Zheng, S.; Lin, H.; Liu, J.-Q.; Balic, M.; Datar, R.; Cote, R. J.; Tai, Y.-C. *J. Chromatogr. A* **2007**, *1162*, 154−161.
(19) Kahn, H. J.; Presta, A.; Yang, L.; Blondal, J.; Trudeau, M.; Lickley, L.; Holloway, C.; McCready, D. R.; Maclean, D.; Marks, A. *Breast Cancer Res. Treat.* **2004**, *86*, 237−247.
(20) Kuo, J. S.; Zhao, Y.; Schiro, P. G.; Ng, L.; Lim, D. S. W.; Shelby, J. P.; Chiu, D. T. *Lab Chip* **2010**, *10*, 837−842.
(21) Pinzani, P.; Salvadori, B.; Simi, L.; Bianchi, S.; Distante, V.; Cataliotti, L.; Pazzagli, M.; Orlando, C. *Hum. Pathol.* **2006**, *37*, 711−718.
(22) Lin, H. K.; Zheng, S.; Williams, A. J.; Balic, M.; Groshen, S.; Scher, H. I.; Fleisher, M.; Stadler, W.; Datar, R. H.; Tai, Y.-C.; Cote, R. J. *Clin. Cancer Res.* **2010**, *16*, 5011−5018.
(23) Coumans, F. A. W.; van Dalum, G.; Beck, M.; Terstappen, L. W. M. M. *PLoS One* **2013**, *8*, e61774.
(24) Schiro, P. G.; Zhao, M.; Kuo, J. S.; Koehler, K. M.; Sabath, D. E.; Chiu, D. T. *Angew. Chem., Int. Ed.* **2012**, *51*, 4618−4622.
(25) Zhao, M.; Schiro, P. G.; Kuo, J. S.; Koehler, K. M.; Sabath, D. E.; Popov, V.; Feng, Q.; Chiu, D. T. *Anal. Chem.* **2013**, *85*, 2465−2471.
(26) Zhao, M.; Nelson, W. C.; Wei, B.; Schiro, P. G.; Hakimi, B. M.; Johnson, E. S.; Anand, R. K.; Gyurkey, G. S.; White, L. M.; Samual, W. H.; Coveler, A. L.; Chiu, D. T. *Anal. Chem.* **2013**, *85*, 9671−9677.
(27) Georgoulias, V.; Bozionelou, V.; Agelaki, S.; Perraki, M.; Apostolaki, S.; Kallergi, G.; Kalbakis, K.; Xyrafas, A.; Mavroudis, D. *Ann. Oncol.* **2012**, *23*, 1744−1750.
(28) Bonnomet, A.; Brysse, A.; Tachsidis, A.; Waltham, M.; Thompson, E. W.; Polette, M.; Gilles, C. *J. Mammary Gland Biol. Neoplasia* **2010**, *15*, 261−273.
(29) Adams, A. A.; Okabare, P. I.; Feng, J.; Hubert, M. L.; Patterson, D.; Gotten, J.; McMarley, R. L.; Nikitopoulos, D.; Murphy, M. C.; Soper, S. C. *J. Am. Chem. Soc.* **2008**, *130*, 8633−8641.
(30) Zhao, M.; Wei, B.; Nelson, W. C.; Schiro, P. G.; Chiu, D. T. *Lab Chip* **2015**, *15*, 3391−3396.

DOI: 10.1021/acs.analchem.5b02241
Anal. Chem. 2015, 87, 9389−9395